Journal of Molecular Structure 1139 (2017) 371–380

Contents lists available at ScienceDirect

Journal of Molecular Structure

journal homepage: http://www.elsevier.com/locate/molstruc

Spectroscopic, molecular docking and structural activity studies of (*E*)-*N*′-(substituted benzylidene/methylene) isonicotinohydrazide derivatives for DNA binding and their biological screening

Nasima Arshad [a, *], Fouzia Perveen [b], Aamer Saeed [c], Pervaiz Ali Channar [c], Shahid Iqbal Farooqi [a], Fayaz Ali Larik [c], Hammad Ismail [d], Bushra Mirza [d]

[a] Department of Chemistry, Allama Iqbal Open University, Islamabad, Pakistan
[b] Research Center for Modeling and Simulations, National University of Sciences and Technology, Islamabad, Pakistan
[c] Department of Chemistry, Quaid-i-Azam University, Islamabad, Pakistan
[d] Department of Biochemistry, Quaid-i-Azam University, Islamabad, Pakistan

ARTICLE INFO

Article history:
Received 10 January 2017
Received in revised form
9 March 2017
Accepted 14 March 2017

Keywords:
Isonicotinohydrazides
UV spectroscopy
Molecular docking
Binding mode
Binding constant
Antitumor activity

ABSTRACT

Acid catalyzed condensation of isoniazid with a number of suitably substituted aromatic and heterocyclic aldehydes was carried out in dry ethanol to afford the title (*E*)-*N*′-(substituted benzylidene/methylene) isonicotinohydrazides (SF 1 – SF 4) in good yields. These compounds were characterized and further investigated for their binding with ds.DNA using UV– spectroscopy and molecular docking and for antitumor and antimicrobial potentials. A good correlation was found among spectroscopic, theoretical and biological results. UV– spectra in the presence of DNA concentrations and their data interpretation in terms binding constant "K_b" and free energy change (ΔG) provided evidences for the significant and spontaneous binding of the compounds with DNA. Molecular docking studies and structural analysis further supported the UV-findings and indicated that the modes of interactions between bromo- (SF 1) and flouro- (SF 4) substituted isonicotinohydrazides is intercalation while methoxy- (SF 2) and hydroxy- (SF 3) substituted isonicotinohydrazides interact with DNA helix via groove binding. SF 1 exhibited comparatively higher K_b value (UV–; 8.07×10^3 M^{-1}, docking; 8.11×10^3 M^{-1}) which inferred that the respective compound muddles to DNA most powerfully. SF 1 has shown the lowest IC_{50} (345.3 μg/mL) value among all the compounds indicating its comparatively highest activity towards tumor inhibition. None of the compound has shown perceptible antibacterial and antifungal activities.

© 2017 Published by Elsevier B.V.

1. Introduction

Hydrazide, an effective class of organic compounds, is known for therapeutic and biological activities [1,2]. Most of the hydrazides have been reported for their anti-fungal, anti-bacterial and anti-inflammatory activities [1–4]. Isoniazid (isonicotinic hydrazide; INH) is one of the primary drugs used in combination with ethanbutol, rifampin, streptomycin and pyrazinamide to treat tuberculosis [5]. Despite the large number of compounds containing the isoniazid moiety which have already been synthesized and tested, there is still a need for new compounds of this kind, due to the increasing resistance of bacterial strains of certain type of antibiotics [6].

The remarkable biological activity of Schiff bases, or the aroyl hydrazones, R–CO–NH–N=CH-R′ and the dependence of their mode of chelation with transition metal ions present in the living system have been of significant interest in the past [7–10]. Isoniazid was treated with different substituted aromatic aldehydes to produce Schiff bases [11]. The coordination compounds of aroyl hydrazones have been reported to act as enzyme inhibitors [12] and are useful due to their pharmacological applications [13,14]. Isoniazid is a drug of proven therapeutic importance and is used against a wide spectrum of bacterial ailments, e.g., tuberculosis [15]. Hydrazones derived from condensation of isoniazid with pyridine aldehydes have been found to show better antitubercular activity than INH [16].

Unfortunately, the actual formulations show several undesired collateral effects and can even cause irreversible damage in the liver in chronic patients. This fact, together with the resistance that microorganisms develop against these drugs, encouraged the search for

* Corresponding author.
E-mail address: nasimaa2006@yahoo.com (N. Arshad).

http://dx.doi.org/10.1016/j.molstruc.2017.03.055
0022-2860/© 2017 Published by Elsevier B.V.

new compounds with therapeutic effects [17,18]. The combination of INH with some hydroxy aldehydes leads to the formation of stable hydrazones that show conserved activity and less toxicity, due to the inactivation of the NH_2 group of INH [13]. In particular, a group of hydrazones has been reported as more effective and efficient anti-tuberculous agents in macrophages than INH itself [14].

Cancer – a leading cause of premature death in the world – can be cured by preventing the rapid proliferation of cancer cells for which the replication of DNA is to be arrested. Antiviral, anticancer, antitumor and antibiotic drugs can easily target nucleic acids [19–21]. Drugs can bind to DNA both covalently (irreversible) as well as non-covalently (reversible via intercalation, grove binding or electrostatic interactions).

Various platinum(II)-based complexes of like cisplatin, oxalylplatin, nedaplatin and carboplatin has achieved clinical status as well known antitumor agents. These drugs targeted DNA primarily via covalent linkage with the nitrogen atoms on DNA bases, mainly N^7 of guanine [22]. However, despite of their high activity towards killing cancer cells, applications are limited by serious disadvantages like poor water solubility, tolerance by the tumor and irreversible covalent binding which may further lead to toxic side effects like alopecia (hair falls out), kidney failure, allergies, hearing loss etc.

Non-covalent binding is reversible and is typically preferred over covalent adduct formation. Since irreversible binders like cisplatin bind quite strongly to the damaged DNA, it has been difficult to achieve similar affinity using small non-covalent binders, and remains a major challenge among researchers to design drugs that bind reversibly with the DNA. Although lot of research has been carried out, but there is still a quest to gain more insight on different aspects of the association of small molecules with DNA in order to obtain highly selective and efficient drug candidates. A verity of intercalators and groove binders are known for their anticancer, antiviral, antitumor, antibacterial and antifungal activities [23]. Kinetic and thermodynamic studies on compound – DNA interaction by using spectroscopic, electrochemical and variety of other techniques have initially provided important physical parameters that may further lead to investigate a compound as a potential drug candidate [1,24–27]. Modes of interactions of a compound with DNA can also be predicted by molecular docking simulation and implication of this theoretical technique along with the assistance of experimental techniques is very helpful for rational drug design [28].

Antimitotic activity of potato disc tissue, in which inhibition of *Agrobacterium tumefaciens*– induced tumors is monitored, can be used to detect antitumor effects in broader range [29]. Potato disc antitumor assay is based on assumption that similar tumorogenic mechanisms occur in both animals and plants [30]. Antitumor screening assays in animals and potato disc antitumor assay have been reported for their good correlation [29]. Antitumor activity of several compounds has been investigated for *A – tumefaciens* induced tumors in potato discs [1,24,27,31].

The enormous therapeutic properties of hydrazides is a key motivation in this studies to synthesize stable and less toxic compounds of INH with suitably substituted aromatic aldehydes and to investigate their interactions with DNA by using spectroscopic and molecular docking techniques and with *A – tumefaciens* induced tumor in potato disc.

2. Experimental

2.1. Materials and methods

All the chemical and reagents used in synthesis, DNA binding procedures and biological assays were of analytical grade. Monitoring of the synthetic reactions was carried out by the thin-layer chromatography (TLC) using silica gel (aluminum card, layer thickness 0.2 mm, HF-254, Riedal-de-Haen) precoated plates and was visualized under UV-lamp. All the necessary purification and drying of solvents were carried out according to standard methods [32]. The dried solvents were stored over molecular sieves. Falcon method was adopted as a protocol to extract double strand (ds.) DNA from chicken blood [33]. All the glassware, Falcon tubes and water used in extraction procedure were autoclaved.

DNA threads were dissolved in water and concentration of stock DNA solution (phosphate groups' molarity) was determined through UV–visible spectroscopy. Absorbance is measured at λ_{max} of 260 nm. Stock DNA concentration was obtained by substituting molar extinction coefficient, $\varepsilon_{260} = 6600\ cm^{-1}M^{-1}$ and absorbance at maximum wavelength in Lambert-Beer's equation ($A = \varepsilon Cl$) [33,34]. DNA absorbance was measured at another wavelength (280 nm) and absorbance ratio A_{260}/A_{280} was evaluated. The value was found greater than 1.8 which assured that the extracted DNA is sufficiently pure and no ambiguity is there for the presence of protein [35]. The stock solutions of synthesized compounds were prepared by dissolving them in 10% aqueous DMSO. For DNA binding studies, compound's concentration was optimized and kept constant while adding various diluted concentrations of DNA at 37 °C. *Agrobacterium tumefaciens* strain (AT-10) and red skinned potatoes were used in antitumor assay, while four bacterial ((ATCC 6538, ATCC 10240, ATCC 15224, ATCC 14028) and four fungal strains (FCBP 0300, FCBP 0198, FCBP 66, FCBP 0291) were used in antimicrobial assays.

2.2. Instrumentations

Melting points were recorded using a digital Gallenkamp (SANYO) model MPD.BM 3.5 apparatus and are uncorrected. ^1H NMR and ^{13}C NMR spectra were determined at 300 MHz using a Bruker AM-300 spectrophotometer in acetone d_6. FTIR spectra were recorded on Bio-Rad-Excalibur Series Mode FTS 3000 MX spectrophotometer (USA) in range of 4000–400 cm^{-1}. Mass Spectra (EI, 70eV) on a GC-MS, Agilent technologies 6890 N and an inert mass selective detector 5973 mass spectrometer technologies. Thin layer chromatography (TLC) was conducted on 0.25 mm silica gel plates (60 F254, Merck). Visualization of chromatograms was made with UV at 365 and 254 nm.

Shimadzu1800 spectrophotometer (TCC-240A, Japan)) armed with temperature control device was used to record the electronic absorption spectra using 1.0 cm matched quartz cells. Hettich EBA20 Portable Centrifuge C 2002 (Max. speed: 6000 min-1) and vortex machine were used for the extraction of DNA from chicken blood. MOE-dock by Chemical Computing Group Inc was used for molecular docking simulation. Molecular modeling studies were performed on Pentium1.6 GHz workstation, 512 MB memory with the Windows Operating System that applies a two stage scoring process to sort out the best conformations and orientations of the ligand based on its interaction pattern with the DNA.

2.3. Synthesis of N′-(substituted benzylidene/methylene) isonicotinohydrazides

Isoniazid (0.5 g, 3.65 mmol) was dissolved in 15 mL of absolute alcohol. The suitable aldehyde (3.70 mmol) was added dropwise with constant stirring in presence of catalytic amount of acetic acid. The reaction mixture was refluxed for 4–6 h and the completion of reaction was monitored by TLC (Petroleum ether: ethyl acetate 4:1). The reaction mixture was cooled and the resulting solid was filtered washed with cold ethanol and finally recrystallized from absolute ethanol.

2.4. Characterization data

2.4.1. (E)-N′-(4-bromobenzylidene)isonicotinohydrazide (SF 1)

Light blue Solid (85%) m.p 142 °C; Rf: 0.78; IR; (KBr, cm^{-1}): 3190 (N–H), 1610 (CN), 1585(Ar-C=C), 1095; ^{1}H NMR (Acetone-d6,300 MHz) δ: 11.54 (bs NH), 8.45 (t, 2H) 7.57 (t, 2H); 7.55 (d, 2H, J = 7.5 Hz, ArH), 7.41 (d, 2H, J = 7.5 Hz, ArH) 7.34 (s, 1H); ^{13}C NMR (75 MHz) δ: 173(C=O),157(C=N), 144(Ar), 140 (Ar), 137 (Ar), 129 (Ar), 128(Ar), 123(Ar), GC-MS (EI, 70 eV): *m/z* (%): 303(21), 154 (65), 106(100).

2.4.2. (E)-N′-(4-methoxybenzylidene)isonicotinohydrazide (SF 2)

yellow Solid (88%) m.p 165 °C; Rf: 0.73; IR; (KBr, cm^{-1}): 3245 (N–H), 1618 (CN), 1585(Ar-C=C), 1077; ^{1}H NMR (Acetone-d6,300 MHz) δ: 11.96 (bs NH), 8.65 (t, 2H) 7.58 (t, 2H); 7.53 (d, 2H, J = 7.5 Hz, ArH), 7.49 (d, 2H, J = 7.5 Hz, ArH) 7.38 (s, 1H); 3.68 (s, 3H); ^{13}C NMR (75 MHz) δ: 189(C=O),169(C=N), 148(Ar), 144 (Ar), 139 (Ar), 137 (Ar), 131(Ar), 129(Ar), 59(0Me), GC-MS (EI, 70 eV): *m/z* (%): 255(16), 107(65), 106(100).

2.4.3. (E)-N′-(2-hydroxybenzylidene)isonicotinohydrazide (SF 3)

yellow Solid (70%) m.p 238 °C; Rf: 0.83; IR; (KBr, cm^{-1}): 3443 (OH), 3243 (N–H), 1615 (CN), 1588(Ar-C=C), 1074; ^{1}H NMR (Acetone-d6,300 MHz) δ: 12.27 (bs 1H), 11.08(bs 1H), 8.77 (t, 2H) 8.68 (s, 1H); 7.82–7.85 (t, 2H), 7.55–7.61 (d, 1H) 7.38 (s, 1H); 7.27–7.33 (t, 1H); 6.89–6.89 (m, 2H); ^{13}C NMR (75 MHz) δ: 179(C=O),169(C=C–OH), 155(C=N), 145(Ar), 140 (Ar), 137 (Ar), 134 (Ar), 129(Ar), 124(Ar), 122(Ar), 120(Ar). GC-MS (EI, 70 eV): *m/z* (%): 241(26), 93(55), 106(100).

2.4.4. (E)-N′-(4-fluorobenzylidene)isonicotinohydrazide (SF 4)

yellow Solid (78%) m.p 145 °C; Rf: 0.65; IR; (KBr, cm^{-1}): 3230 (N–H), 1600 (CN), 1575(Ar-C=C), 1075; ^{1}H NMR (Acetone-d6,300 MHz) δ: 11.66 (bs NH), 8.55 (t, 2H) 7.62 (t, 2H); 7.57 (d, 2H, J = 7.5 Hz, ArH), 7.50 (d, 2H, J = 7.5 Hz, ArH) 7.44 (s, 1H); ^{13}C NMR (75 MHz) δ: 179(C=O),165(C=N), 146(Ar), 141 (Ar), 136 (Ar), 132 (Ar), 129(Ar), 127(Ar), GC-MS (EI, 70 eV): *m/z* (%): 243(16), 94 (65), 106(100).

2.5. Procedure for analysis

2.5.1. UV–visible spectroscopic titrations

DNA concentration at 260 nm was evaluated 6.5×10^{-5} M. Spectroscopic titrations were done at 37 °C (human body temperature). The concentration of each synthesized compound (SF 1 – SF 4) was optimized and prepared as 1.14×10^{-4} M. Absorbance measurements were performed by keeping the concentration of synthesized compounds (SF 1 – SF 4) constant (1.14×10^{-4} M) in the sample cuvette, while varying the concentration of ds.DNA from 10 μM to 70 μM. Before running the spectra for absorbance measurement, each solution was allowed to stay for few minutes so that equilibrium could be achieved between compound and DNA during complex formation. Sample solutions were further kept for few seconds within the cell cavity to assure the required temperature (37 °C).

2.5.2. Molecular docking method

Ligand molecules (SF 1 – SF 4), were drawn and minimized on MOE window using MOE builder and entered into MOE database. The starting point of the docking simulation was the X-ray structure of the DNA with PDB ID 1BNA obtained through the protein data bank (PDB) and imported to MOE window. All water molecules were removed from the complex with 12 base pairs running in 5′-3′ direction. The base pair sequence was (5′-D(CGCGAATTCGCG)-3′): (5′-D(CGCGAATTCGCG)-3′) with molecular weight of 7326.84. All hydrogen atoms were added to the structure with their standard geometry followed by their energy optimization tool using MOPAC 7.0. The resulting DNA model was subjected to systematic conformational search at default parameters with RMS gradient of 0.01 kcal mol^{-1} using Site Finder. A number of runs were carried out to get a final binding docking pose as accurate as possible. The best conformation was selected based on energetic ground and the minimum Final Docking Energy (ΔG) [36,37].

2.5.3. Potato disc antitumor assay

Agrobacterium tumefaciens strain (AT-10) was used in this assay as inoculums with the final concentrations of 1000, 100, 10 μg/mL of each test compound respectively [38]. The surface of red skinned potato was sterilized with 0.1% $HgCl_2$ and their cylinders were prepared with the help of sterilized cork borer. These cylinders were cut in to 5 × 8 mm discs and ten discs were placed on each solidified agar plate. Then 50 μL of inoculums was added to the top of each disc and each petriplate was wrapped with parafilm strips to avoid contamination and loss of moisture during incubation period. These petriplates were then incubated at 28 °C. After 21 days number of tumors was counted after staining with the Lugol's solution (10% KI and 5% I_2). Vincristine sulphate and DMSO were used as positive and negative control respectively. Each experiment was repeated three times and IC_{50} values for each compound were evaluated. Percentage inhibition was calculated by the following formula;

$$\% \text{ inhibition} = 100 - \left(\frac{\text{Number of tumors in test compound}}{\text{Number of tumors in negative control}}\right) \times 100$$

2.5.4. Antimicrobial assay

Antibacterial and antifungal activities of the test compounds were studied by employing disc diffusion method. Four bacterial strains; 2 g positive *Staphylococcus aureus* (ATCC 6538) and *Micrococcus luteus* (ATCC 10240) and 2 g negative *Escherichia coli* (ATCC 15224) and *Salmonella typhimurium*(ATCC 14028) for antibacterial while four fungal strains; *Mucor species* (FCBP 0300), *Aspergillusniger* (FCBP 0198), *Aspergillusfumigatus* (FCBP 66) and *Fusariumsolani* (FCBP 0291) were used in the this method [39,40].

In antibacterial assay, organisms were cultured in nutrient broth at 37 °C for 24 h. 10^6 colony-forming units (CFU/mL) of test strain was added to nutrient agar medium at 45 °C and poured into sterile petri plates. The medium was allowed to solidify. 5 μL of each test compound with 200 μg/mL final concentration were poured on 4 mm sterile paper discs separately and placed on nutrient ager plates. In each plate DMSO served as negative control and Kanamycin served as positive control. Plates were incubated at 37 °C for 24 h. The antibacterial activity was determined by measuring the diameter of zones showing complete inhibition (mm).

In antifungal assay, organisms were cultured on sabouraud dextrose agar (SDA) at 28 °C for 24 h. Autoclaved broth culture (3 mL) was allowed to cool down to 45 °C and poured into sterile petri plates. 5 μL of each test compound with 200 μg/mL final concentration were poured on 4 mm sterile paper discs separately and placed on SDA plates. The discs supplemented with DMSO and Terbinafine were used as negative and positive control, respectively. Plates were incubated at 28 °C for seven days and fungal growth was determined by measuring growth diameter (mm) and growth inhibition was calculated with reference to the controls.

3. Results and discussion

3.1. Synthetic pathway and physical description

Synthesis of the title compounds (SF 1 – SF 4) was carried out according to synthetic route given in Scheme 1 [41,42]. Thus isoniazid was condensed with a number of suitably substituted aromatic aldehydes in dry ethanol to afford the title compounds (SF 1– SF 4) in good yields.

IR spectra of the synthesized compounds were recorded in the range 4000 cm^{-1} – 400 cm^{-1} and important bands are given along the synthesis in the experimental section. The synthesis of compounds SF 1 to SF 4 was indicated in the IR spectra by the presence of two strong peaks 3243 cm^{-1} and 1585 cm^{-1} that were assigned to N–H and aromatic sp^2 hybridized C=C vibrations. The absorption for carbonyl group appeared between 1700 cm^{-1} – 1720 cm^{-1}. Appearance of C=N band at 1610 cm^{-1} in the FTIR spectra confirmed the formation of Schiff bases.

Broad singlet of the –NH– group of hydrazone in the range of δ 12.26 ppm – δ 11.87 ppm in ^{1}H NMR confirmed the formation of imine linkage. Two sets of protons of 4-substituted pyridine ring shows two triplets at δ 8.75 ppm and δ 7.74 ppm. Yields of the products depend on the nature of aldehyde used for condensation. The aldehydes with electron withdrawing groups are more reactive and give good yields compared to those with electron releasing groups.

3.2. Absorption spectra of synthesized compounds

Initially, UV–visible spectra of four pure isonicotinohydrazides (SF1 – SF 4) were recorded in 10% aqueous DMSO in a complete UV–visible range (200 nm–800 nm). The solution of each compound was kept at lower concentration so that only internal transitions ($\pi - \pi^*$; $n - \pi^*$) of the ligand itself and its complexes could be observed in UV- region. A single intense peak of the compounds; SF 1, SF 2, SF 3 and SF 4 was observed in UV- region at 303 nm, 319 nm, 329 nm and 310 nm, respectively.

Further, spectral responses were recorded separately using various concentrations of each compound in increasing dilution range. Absorbance for each concentration at λ_{max} was plotted against concentrations, Fig. 1. Absorbance increases linearly with concentration for all the compounds as evident from their linear regression values; $R^2 = 0.989, 0.974, 0.981, 0.992$ respectively for SF 1, SF 2, SF 3 and SF 4.

Molar extinction coefficient (ε) were evaluated from slope values as; 10400 $cm^{-1}M^{-1}$, 37054 $cm^{-1}M^{-1}$, 9200 $cm^{-1}M^{-1}$, 22800 $cm^{-1}M^{-1}$ respectively for SF 1, SF 2, SF 3 and SF 4. Burawoy classification presumes that K band (also called electron transfer or ET–band) are responsible for $\pi - \pi^*$ transitions in a compound involving a conjugation group and when a group on aromatic ring has non-bonded electron pairs; $n - \pi^*$ transitions occur from R band. The observed values of λ_{max} which were in the range of 300 nm–350 nm and the values of molar extinction coefficients predict that K band for $\pi - \pi^*$ and R band for $n - \pi^*$ transitions are operative for all compounds [43].

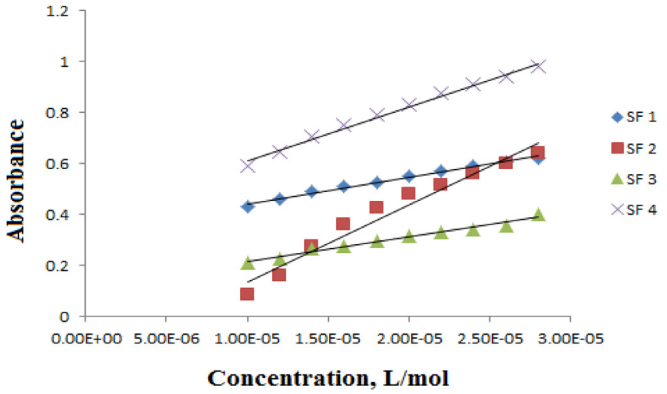

Fig. 1. Concentration profiles of the compounds.

3.3. DNA binding study by UV–spectroscopy

Drug – DNA investigations by electronic absorption spectroscopy provides a valuable complement to other techniques used for DNA binding studies [24]. Commonly, intercalation is considered more obvious mode for strong interaction and a compound intercalating within DNA base pairs has been associated with hypo/hyper-chromism along with a pronounced red/or blue shift as observed in the absorption spectra of compound – DNA complex [44–47]. In addition, increase/or decrease in the absorption peak intensity with no/or unnoticeable shifting of the wavelength in the absorption spectra of small molecules is characterized as electrostatic or groove binding interaction mode [46].

UV–spectra of four isonicotinohydrazides were recorded separately by adding varying concentrations (10 μM–70 μM) of DNA and concentration effect of DNA on optimized concentration (1.14×10^{-4} M) of all the compounds was observed at body temperature (37 °C), Fig. 2. Addition of DNA in aliquots was resulted in decrease in absorption peak intensity of the compounds with a blue

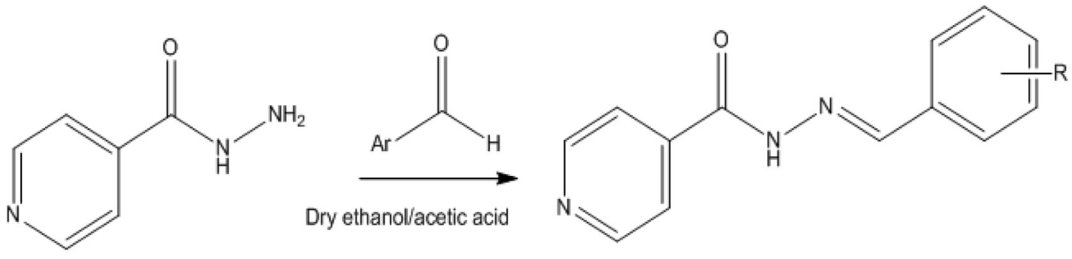

R-	
SF 1	4-bromo
SF 2	4-Methoxy
SF 3	2-Hydroxy
SF 4	4-flouro

Scheme 1. Synthetic route to *N'*-(substituted benzylidene/methylene) isonicotinohydrazides (SF 1 – SF 4).

shift of 2.4 nm, 0.6 nm, 0.4 nm and 2.1 nm respectively for compounds SF 1, SF 2, SF 3 and SF 4 respectively. Percent decrease in the peak intensities of SF 1, SF 2, SF 3 and SF 4 in the presence of DNA was evaluated as 20.2%, 23.8%, 22.5%, 32.7% respectively using following equation;

$$H\% = \frac{A_{free} - A_{bound}}{A_{free}} \times 100$$

The observed hyporchromic effect along with blue shift may be designated to the binding of the compounds with ds.DNA through intercalative mode of interaction [24,48,49]. Decrease in the peak intensity is related to decreasing transition probabilities as coupling π–orbital is partially filled by electrons which is consequence of hypochromism in the spectra [43,50]. On the other hand, a blue shift arises in the spectra due to improper coupling (conformational changes) of π^*– orbital of intercalated part of the compound with the π– orbital of the base pairs [43]. This distortion in the π – orbital of the base pairs and π^*– orbital of intercalated molecules resulted in unstacking of base pairs with hypsochromic shift. However, measured blue shifts in the compounds' spectra SF 2 (0.6 nm) and SF 3 (0.4 nm) after DNA addition were very slight and could be ignored. Hence observed spectral changes in SF 2 and SF 3 after the addition of DNA may be attributed to either external interaction via electrostatic interaction or groove binding [46,51,52].

An isosbestic point was also observed for all compounds' spectra, Fig. 2, which assured that no other species except investigated compound and its DNA complex are present in the reaction mixture and equilibrium is established between bound DNA and free form of the compound [24,27,53].

Determination of binding constants and free energy changes of compound – DNA complexes.

Variation in absorbance of a compound in UV–spectra upon DNA addition lead to evaluate the binding constant *"K_b"* of compound – DNA complex using Benesi – Hildebrand equation [54].

$$\frac{A_o}{A - A_o} = \frac{\varepsilon_G}{\varepsilon_{H-G} - \varepsilon_G} + \frac{\varepsilon_G}{\varepsilon_{H-G} - \varepsilon_G} \frac{1}{K_b[DNA]} \quad (1)$$

Where, K_b is the binding constant, A_o and A are the absorbance of free and DNA–bound complex, ε_G and $\varepsilon_{H\text{-}G}$ are their molar extinction coefficients respectively. From the plot of $A_o/(A\text{-}A_o)$ against *1/[DNA]*, ratio of the intercept to the slope furnished the value of binding constant, K_b, Fig. 3.

Binding constant values (K_b) were evaluated for all the four compounds under physiological temperature (37 °C) and given in Table 1. K_b values for all compounds with DNA were found in the order of magnitude 10^3 M^{-1} which is same binding order as reported for intercalators – isoxazocucumine and 4-aminophenazone Schiff bases (4-{(3,4,5-trimethoxybenzylidine) amino}phenazone and 4-{(4-chlorobenzylidine)amino} phenazone) and depicted significant interactions of all the four isonicotinohydrazides with the DNA [55,56]. UV–spectral changes

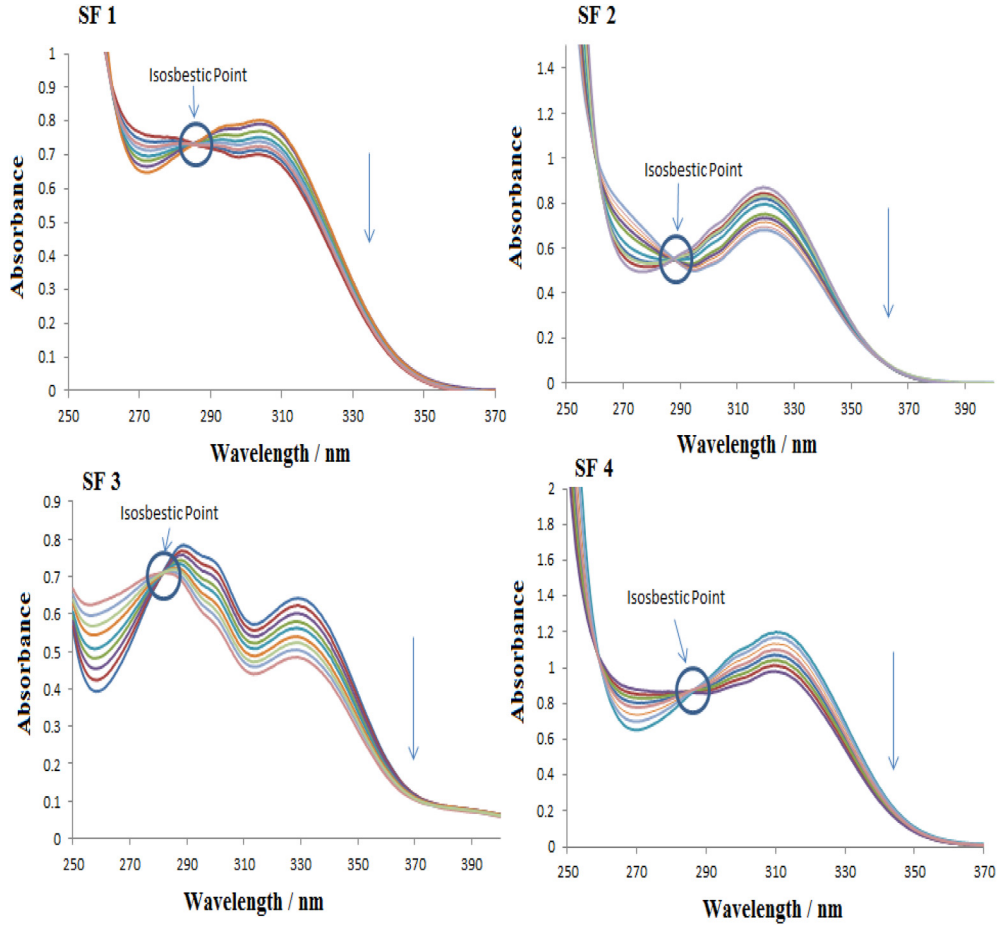

Fig. 2. UV–Spectra for SF 1, SF 2, SF 3 and SF 4 (1.14×10^{-4} M) without and in the presence of 10 μM (b), 20 μM (c), 30 μM (d), 40 μM (e), 50 μM (f), 60 μM (g) and 70 μM (h) DNA at 37 °C. The downward arrow direction indicates increasing concentrations of DNA.

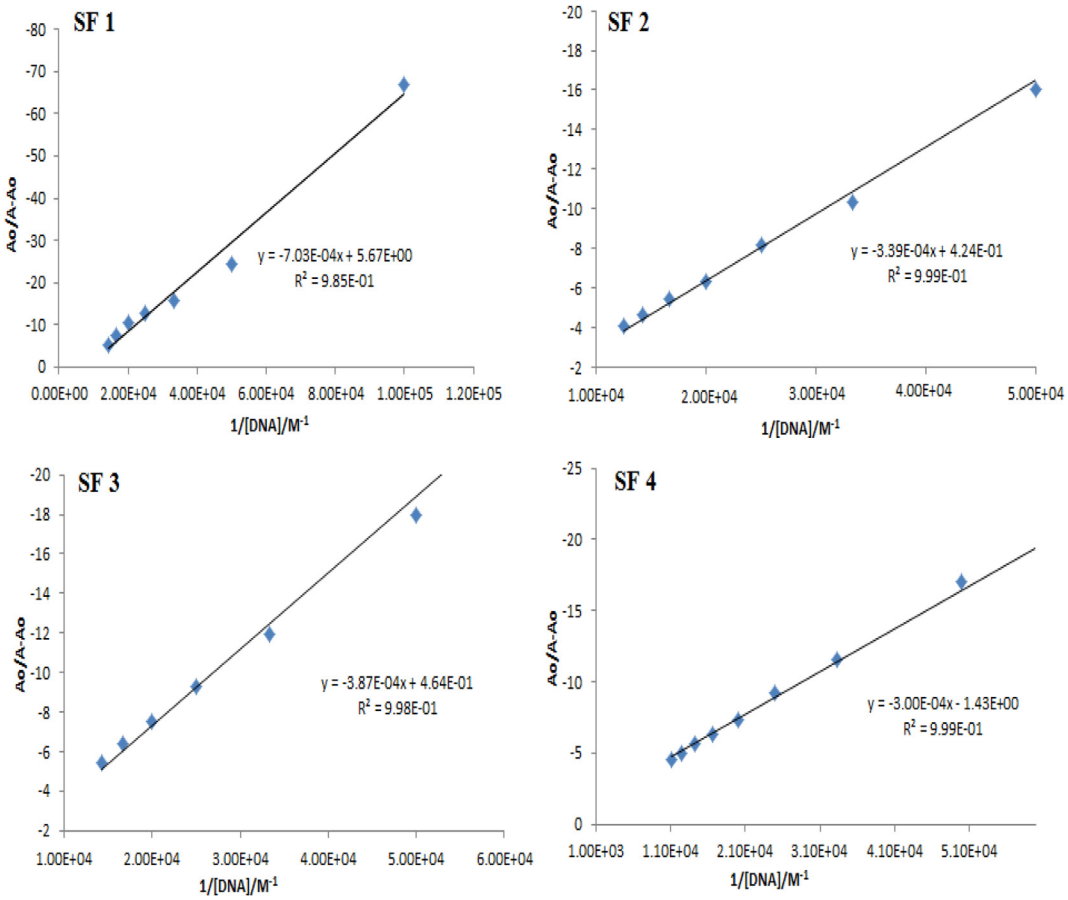

Fig. 3. Plot of $A_o/A\text{-}A_o$ *vs.* 1/[DNA] for the application of Benesi-Hildebrand equation for calculation of compound – DNA binding constant at 37 °C.

Table 1
Binding constants and free energy values for the isonicotinohydrazides – DNA complexes from UV– spectrophotometric and molecular docking data.

Complex code	UV– spectroscopy		Molecular docking	
	"K_b"/M^{-1}	$^{-}\Delta G$/kjmol^{-1}	"K_b"/M^{-1}	$-\Delta G$/kjmol^{-1}
SF 1–DNA	8.07×10^3	23.20	8.11×10^3	23.16
SF 2–DNA	1.25×10^3	18.38	6.25×10^2	15.94
SF 3–DNA	1.20×10^3	18.27	3.19×10^2	14.28
SF 4–DNA	4.76×10^3	21.82	3.94×10^3	20.51

observed during isonicotinohydrazides – DNA complex formation *i.e.,* decrease in peak intensity and blue shift in compounds' spectra may further be credited to small structure of isonicotinohydrazides molecules whose planer parts may possibility be intercalated between the adjacent DNA base pairs. K_b order magnitude (10^3 M^{-1}) has also been reported for electrostatic interaction or groove binding in various studies [51,52]. Since order of magnitude is same for all the compounds i.e., 10^3 M^{-1}; on the basis of K_b values and spectral effects, compounds SF 1 and SF 4 may be designated as intercalators, while compounds SF 2 and SF 3 may be assigned as groove binders.

As binding constant "K_b" measures complex stability, the values evaluated for all the synthesized compounds for their binding with DNA were found significant and may infer to the formation of stable compound – DNA complex. Compound SF 1 showed comparatively greater K_b value (8.07×10^3 M^{-1}) not only among the investigated compounds but also this value was found greater than that reported for the intercalator– isoxazocucumine (6.3×10^3 M^{-1}) [55].

The order of binding constants of four isonicotinohydrazides was as follows;

$$K_{b(SF\ 1)} > K_{b(SF\ 4)} > K_{b(SF\ 2)} > K_{b(SF\ 3)}$$

Further, Gibbs free energies (ΔG) of isonicotinohydrazides – DNA complexes were calculated by using the values of binding constant (K_b) in classical vant Hoff's equation;

$$\Delta G = -RT\ln K_b \quad (2)$$

Free energy changes were evaluated as negative values indicating that all isonicotinohydrazides interacted spontaneously with DNA during compound – DNA adducts formation, Table 1. However, for compound SF 1, ΔG was evaluated more negative as compared to other compounds attributing comparatively more spontaneity of its binging with DNA, Table 1. The order of complex spontaneity was same as for binding constant.

$$\Delta_{GSF\ 1} > \Delta_{GSF\ 4} > \Delta_{GSF\ 2} > \Delta_{GSF\ 3}$$

3.4. Computational structural analysis and molecular docking studies

The geometries of four compounds (SF 1, SF 2, SF 3 and SF 4) were fully optimized with the PM3 semi-empirical electronic structure method and the optimized geometries of four compounds are shown in http://www.scielo.br/scielo.php?script=sci_arttext&pid=S0103-50532012000400009 Fig. 4 (A–D). Optimized

structures indicated that all compounds have planar geometry which is property of an intercalator, but ring A is 122° out of plane, Fig. 4(E), which renders a twist to the structure to develop interactions with groove of the DNA. Optimized geometries of these complexes are similar as shown by superimposed structures in Fig. 4(F), except for the points of interaction with the DNA base pairs, hence binding position of all SF compounds depends upon the nature of substituent attached. Such structural effects have also been reported for netropsin, distamycin and hoescht drugs which positioned differently in grooves based on selective bonding with the hydrogen of DNA bases [57]. In all SF compounds, nitrogen atom on the ring A has the most negative charge (−0.620) that could make bond with hydrogen of DNA base pairs while planar part of the molecule partially intercalates between the DNA base pairs.

In an effort to interpret the molecular mechanism for the interactions of isonicotinohydrazides (SF 1 − SF 4) with DNA, molecular docking was performed to simulate the modes of interactions between the drugs and DNA. The conformations of compounds with lowest free energy are shown in Fig. 5 and electronic descriptors calculated from molecular docking data are given in Table 2. Pose view analysis was also performed. "K_b" and ΔG values for all the compounds were calculated and given in Table 1.

Partial intercalation mode of interaction of SF 1 and SF 4 with 1BNA is explained in Fig. 5 SF 1(a) and Fig. 5 SF 4(a). Bromo- and flouro-substituted aromatic rings intercalates between adjacent base pairs where rest of its structure has flexibility to rotate and develop interactions with DNA backbone. In Fig. 5 SF 1(b) dotted line shows solvent contact and blue blurred regions explain direct

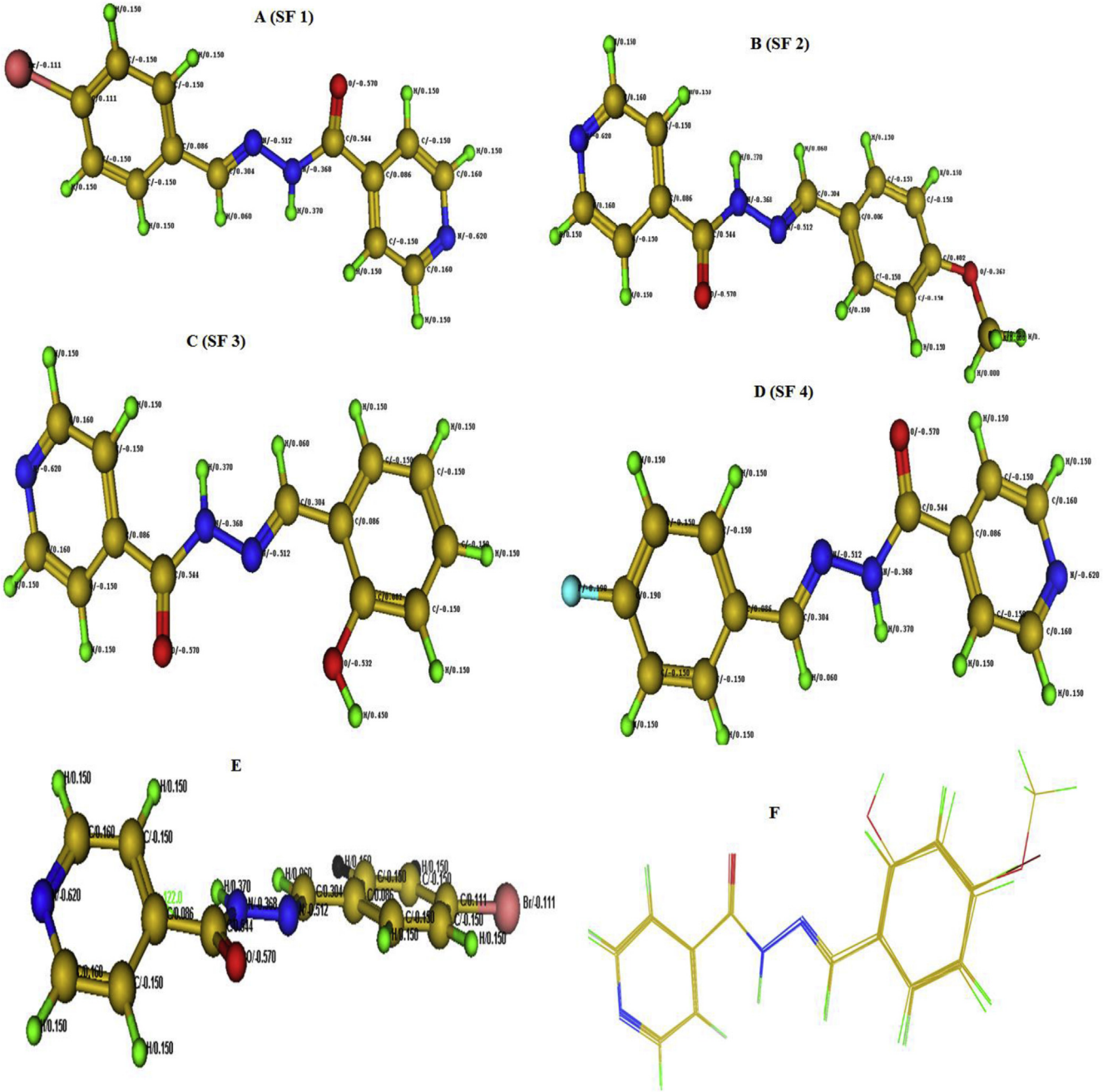

Fig. 4. Optimized structures of SF 1, SF 2, SF 3, SF 4 (A–D), twist structure (E) and superimposed structures (F).

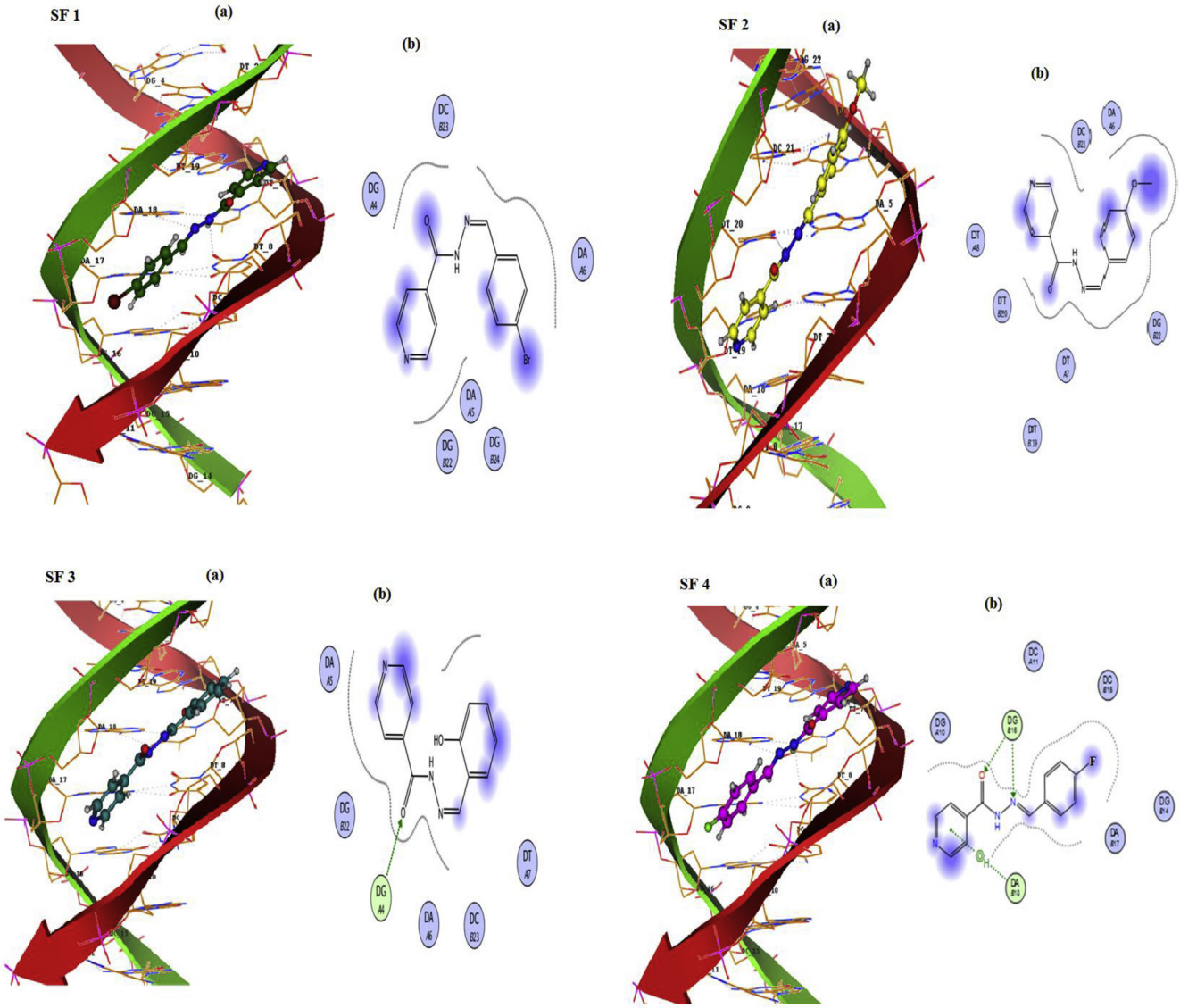

Fig. 5. Molecular docked complex of SF 1, SF 2, SF 3 and SF 4 with IBNA 3D complex (a); 2D lig plot showing interactions of compounds with base pairs of 1BNA (b).

exposure of the ligand to hydrophobic core of 1BNA. Highest value of K_b was evaluated for SF1 which is related to its highest van der Waal's area as compared to other analogues, Table 1.

Methoxy- (SF 2) and hydroxyl- (SF 3) substituted hydrazides interact with 1BNA via groove binding as shown in Fig. 5. Groove binding makes intimate contacts with the walls of the groove as a result of electrostatic and hydrophobic interactions between a drug and DNA bases and its phosphate backbone. SF 3 showed one hydrogen bond between O of SF 3 and H of DG16(labelled green) with bond length 2.88 Å which may renders its greater binding strength. However, 2D lig plot of SF 2 showed that the electronic cloud of adjacent base pairs overlap with the electronic clouds of SF 2 due to which SF 2 was completely entrapped by the DNA base pairs, hence making its binding strength comparatively greater than SF 3.

3.5. Drug –Likeness of isonicotinohydrazides

Pharmacological behavior of the compounds (SF 1– SF 4) was determined theoretically using Lipinski's rule of five criteria [58].

Table 2
Electronic descriptors calculated from molecular docking data.

Complexes	E_{HOMO} kcal/mol	E_{LUMO} kcal/mol	E_{ele} kcal/mol	E_{vander} kcal/mol	E_{IP} kcal/mol	E_{Total} kcal/mol
SF1-1BNA	−9.01	−0.79	−387657.6	269.4	9.11	−71355.8
SF2-1BNA	−8.68	−0.64	−428931.3	266.6	8.68	−74497.6
SF3-1BNA	−8.85	−0.42	−397504.4	247.2	8.85	−70916.4
SF4-1BNA	−9.11	−0.80	−394748.3	241.6	9.01	−74394.5

Table 3
Steric descriptors calculated from molecular docking data.

Complexes	H_f kcal/mol	M_r	S logP	V_{surf}	Dipole	HB donor atoms	HB acceptor atoms	Molar mass g/mol
SF1-1BNA	76.85	7.43	2.61	269.4	3.83	1.00	3.00	304.15
SF2-1BNA	28.19	6.84	1.85	266.6	4.81	1.00	3.00	255.28
SF3-1BNA	26.99	6.75	1.55	247.2	4.40	1.00	3.00	241.25
SF4-1BNA	33.83	7.34	1.98	241.6	3.91	1.00	3.00	243.24

Table 4
Potato disc antitumor activity of the compounds.

Compound code	Percentage inhibition			IC_{50} value (μg/mL)
	1000 μg/mL	100 μg/mL	10 μg/mL	
SF 1	63.5	21.1	5.9	345.3
SF 2	58.9	10.2	0.0	698.3
SF 3	55.7	16.5	2.1	944.5
SF 4	51.4	15.8	1.5	592.2
Vincristine sulphate	100	100	10.7	5.5

The calculated parameters are given in Table 3. All the compounds were found to have HB (hydrogen bond) donor atoms < 5 (the total number of nitrogen–hydrogen and oxygen–hydrogen bonds), HB acceptor atoms < 10 (all nitrogen or oxygen atoms), molecular mass < 500 g/mol and octanol-water partition coefficient S logP < 5. These values were in accordance with Lipinski' criteria for a compound to behave like a drug. However, M_R (molar refractivity) values were evaluated < 10 which are lesser than Lipinski's limits i.e., 40–130. Since, an orally active drug has no more than one violation of the five criteria, compounds SF 1, SF 2, SF 3 and SF 4 can be interpreted to exhibit drug like characteristics and could be administered as drugs after pharmacologically testing.

3.6. Potato disc antitumor study

The results of antitumor assay for the synthesized compounds are given in Table 4 which showed that all of the tested compounds have some activity in tumor inhibition. The highest activity was observed for the compound SF 1 which showed 63.5% tumor inhibition at 1000 μg/mL with the IC_{50} value; 345.3 μg/mL, Fig. 6. Compound SF 3 (IC_{50}: 944.5 μg/mL) was found least active in the reduction of tumor caused by *Agrobacterium tumefaciens*, while compounds SF 2 and SF 4 showed moderated behavior in tumor inhibition mechanism. Order of antitumor potentials of all the compounds was found same as for binding constant, K_b, values attributing a similar correlation between quantitative findings through chemical, theoretical and biological analysis.

$$IC_{50\ (SF\ 1)} < IC_{50\ (SF\ 4)} < IC_{50\ (SF\ 2))} < IC_{50\ (SF\ 3)}$$

3.7. Antimicrobial studies

Using disc diffusion method, each experiment was performed in triplicate to monitor compounds for their antibacterial and antifungal activities. However, measurement of the zone's diameter and growth inhibition results calculated with reference to positive control inferred none of the compound having notable bacterial and fungal inhibition activities.

3.8. Structure – activity relationship

Chemical structure of series of compounds can be related to biological activity through structure – activity relationship (SAR). The effect of a substituent depends both on its nature as well as its position in a compound. In present studies, following order for DNA binding and antitumor activities has been observed;

$$SF\ 1 > SF\ 4 > SF\ 2 > SF\ 3$$

Results indicated that presence of bromo-at the para position of phenyl ring in compound SF1 imparts its highest activity while comparing it with SF 4 having a 4-fluoro group, the activity is significantly reduced. This can be related to the low electronegativity of bromine compared to fluorine which makes the carbon – bromine bond weaker. In addition, higher van der Waals radius of the bromine makes it more lipophilic than fluorine. In the same way, owing to the presence of the ether linkage in O–CH_3 (found in SF 2) renders it less polarity and more lipophilicity compared to the free O–H group present in SF 3. Thus the results can be explained on the basis of order of lipophilicity. SAR depends upon large number of factors, however, in present studies positional effect of the substituent was explained in terms of electronegativity, radius and lipophilicity.

Establishing structure-activity relationship from molecular docking studies, electron donor character of a compound increases as E_{HOMO} increases, while electron accepting character of the compounds increases as its E_{LUMO} decreases. Compound SF 4 is more electron accepting as compared to SF 1 as shown in Fig. 5(b) where two electrons from guanine base pairs are transferred to N and O atom of SF 4. Furthermore, all the four halogens are capable of acting as XB donors (as proven through theoretical and experimental data) and participate in halogen bonding and follow the

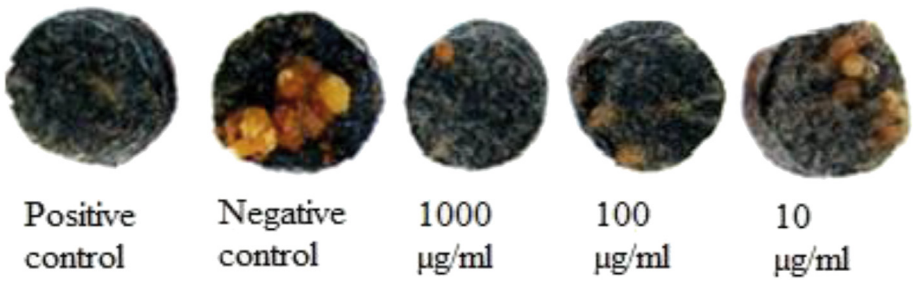

Fig. 6. Effect of compound SF 1 at different concentrations (1000, 100 and10 μg/mL), on inhibition of tumor formation, along with Vincristine sulphate (positive control) and DMSO (negative control) for comparison.

general trend: F < Cl < Br < I, with iodine normally forming the strongest interactions and fluorine forming weakest interactions [59]. Based on general trend of halogens in binding and the values of E_{HOMO} and E_{LUMO}, SF 4 showed strong electron acceptor character as compared to SF 1. E_{HOMO} values for AT (adenine thymine) and GC (guanine cytosine) are −8.64 and −7.35 respectively [60], confirming that in a process of interaction with SF 1, SF 2, SF 3 and SF 4, AT and GC base pairs act as electron donor. Since binding strength decreases as electron donor character of a compound decreases, SF 4 has smaller value of binding constant as compared to SF 1 while interacting with DNA, Table 1.

4. Conclusions

(*E*)-*N*′-(substituted benzylidene/methylene) isonicotinohydrazides (SF 1 − SF 4) were synthesized, characterized, and studied spectrochemically and theoretically for DNA binding and biological activities. Experimental and theoretical investigations have shown SF 1 and SF 4 as intercalators and SF 2 and SF 3 as groove binders. Among all the compounds, SF 1 showed greater K_b and lowest ΔG and IC_{50} values, attributing comparatively strong and spontaneous binding with DNA and greater antitumor potential, respectively. However, no significant bacterial and fungal inhibition activities have been observed for all the compounds. Spectroscopic and docking results of compounds for DNA binding and biological findings have shown good correlation and justified in the present studies. These correlations are often helpful to understand mechanism of drug action on DNA and may lead to explore novel and efficient drug candidates.

Conflict of interest

The authors would like to disclose that no any actual or potential conflict of interest including any financial, personal or other relationships with other people or organizations does exist for the submitted work.

Acknowledgements

This work is supported by Department of Chemistry, Faculty of Science, Allama Iqbal Open University with the help Chemistry, Biochemistry departments of Quaid-i-Azam University and Research Center for Modeling and Simulations, NUST, Islamabad Pakistan.

Appendix A. Supplementary data

Supplementary data related to this article can be found at http://dx.doi.org/10.1016/j.molstruc.2017.03.055.

References

[1] N. Arshad, U. Yunus, S. Razzque, M. Khan, S. Saleem, B. Mirza, N. Rashid, Eur. J. Med. Chem. 47 (2012) 452–461.
[2] A. Özdemir, G. Turan-Zitouni, Z.A. Kaplancikli, Y.J. Tunali, J. Enzyme Inhib, Med. Chem. 3 (2009) 825–831.
[3] A.G. Shadia, H.H. Khaled, S. Ahmed, M.L. Kassab, S.M. Rodriguez, A.A. Kerwin, H.I.D. El-Khamry, Eur. J. Med. Chem. 44 (2009) 1505–1508.
[4] H.M. Abdel-Rahman, M.A. Hussein, Arch. Pharm. 339 (2006) 378–387.
[5] M.C. Raviglione, C. Dy, S. Schmidt, A. Kochi, Lancet 350 (1997) 624–629.
[6] S. Ojha, A. Bapna, G.L. Talesara, Arkivoc 11 (2008) 112–122.
[7] R.C. Aggarwal, N.K. Singh, R.P. Singh, Inorg. Chem. 20 (1981) 2794–2798.
[8] I.A. Tossadis, C.A. Bolos, P.N. Aslanidis, G.A. Katsoulos, Inorg. Chim. Acta 133 (1987) 275–280.
[9] J.A. Anten, D. Nicholis, J.M. Markpoulos, O. Markopoulou, Polyhedron 6 (1987) 1075–1080.
[10] A. Maiti, S. Ghosh, Indian J. Chem. 28A (1989), 980 − 893.
[11] M. Conli, R. Gulielmetli, J. Metzger, Bull. Soc. Chim. Fr. 8 (1967) 2834–2841.
[12] J. Cymerman-Craig, D. Willis, Nature 176 (1955) 34–35.
[13] A. Zubrys, C.O. Siebenmann, Can. J. Chem. 33 (1955) 11–14.
[14] R. Maccari, R. Ottanà, M.G. Vigorita, Bioorg. Med. Chem. Lett. 15 (2005) 2509–2513.
[15] H.H. Fox, Science 116 (1952) 129–134.
[16] S. Kakimoto, K. Yashamoto, Pharm. Bull. 4 (1956) 4–6.
[17] C.M. Nolan, S.V. Goldberg, Int. J. Tuberc. Lung Dis. 6 (2002) 952–958.
[18] S. Keshavjee, I.Y. Gelmanova, P.E. Farmer, et al., Lancet 372 (2008) 1403–1409.
[19] M. Motilal, S.K. Gopinatha, J. Nucleic Acids 23 (2010) 408–593.
[20] M.J. Waring, Annu. Rev. Biochem. 50 (1981) 159–192.
[21] L.H. Hurley, Biochem. Soc. Trans. 29 (2001) 692–696.
[22] G.B. Onoa, G. Cervantes, V. Moreno, M.J. Prieto, Nucleic Acids Res. 26 (1998) 1473–1480.
[23] C.T. Winston, L.B. Dale, Chem. Biol. 11 (2004) 1607–1617.
[24] N. Arshad, M.H. Bhatti, S.I. Farooqi, S. Saleem, B. Mirza, Arab. J. Chem. 9 (2016) 451–462.
[25] D.K. Jangir, S. Charak, R. Mehrotra, S. Kundu, J. Photochem. Photobiol. B Biol. 105 (2011) 143–148.
[26] A. Meenongwa, R.F. Brissos, C. Soikum, P. Chaveerach, P. Gamez, Y. Trongpanich, U. Chaveerach, New. J. Chem. 18 (2016) 28–37.
[27] N. Arshad, S.I. Farooqi, M.H. Bhatti, S. Saleem, B. Mirza, J. Photochem. Photobiol. B Biol. 125 (2013) 70–82.
[28] N. Shahabadi, M. Falsafi, Spectrochim. Acta A Mol. Biomol. Spectrosc. 125 (2014) 154–159.
[29] J.L. McLaughlin, L.L Rogers, Drug. Inf. J. 32 (1998) 513–524.
[30] P.S. Coker, J. Radecke, C. Guy, N.D. Camper, Phytomedicine 10 (2003) 133–138.
[31] A.U. Redman, M.I. Choudhary, W.J. Thomsen, Bioassay Techniques for Drug Development, Harwood Academic Publishers, Amsterdam; The Netherlands, 2001.
[32] D.B.G. Williams, M. Lawton, J. Org. Chem. 75 (2010) 8351–8354.
[33] T. Maniatis, E.F. Fritsch, J. Sambrook, Molecular Cloning: a Laboratory Manual, 1989 (Cold Spring Harbor, New York.
[34] M.E. Reichmann, S.A. Rice, A. Thomas, P. Doty, J. Am. Chem. Soc. 76 (1954) 3047–3053.
[35] S.S. Babkina, N.A. Ulakhovich, Anal. Chem. 77 (2005) 5678–5685.
[36] M.K. Abdel-Hamid, A.A. Abdel-Hafez, N.A. El-Koussi, N.M. Mahfouz, A. Innocenti, C.T. Supuran, Bioorg. Med. Chem. 15 (2007) 6975–6984.
[37] G. Patrick, Medicinal Chemistry by, Department of Chemistry and Chemical Engineering, fourth ed., Paisely University Paisley, Scotland, 2009.
[38] H. Ismail, B. Mirza, I.U. Haq, M. Shabbir, Z. Akhter, A. Basharat, J. Chem. 2015 (2015) 9.
[39] A. Felten, B. Grandry, P.H. Lagrange, I. Casin, J. Clin, Microbiol. 40 (2002) 2766–2771.
[40] M.A. Abbasi, N. Raza, A. Rehman, S. Rasool, K.M. Khan, M. Ashraf, U. Alam, R. Nasar, World J. Pharm. Sci. 2 (2014) 161–169.
[41] P. Ramadevi, R. Singh, A. Prajapati, S. Chakraborty, Adv. Chem. 2014 (2014) 14.
[42] V. Desai, R. Shinde, Inter. J. Pharm. 5 (2015) 930–935.
[43] N. Arshad, N. Abbas, M.H. Bhatti, N. Rashid, M.N. Tahir, S. Saleem, B. Mirza, J. Photochem. Photobiol. B Biol. 117 (2012) 228–239.
[44] S. Usha, I.M. Johnson, R. Malathi, Mol. Cell Biochem. 284 (2006) 57–64.
[45] Y. Sun, S. Bi, D. Song, C. Qiao, D. Mu, H. Zhang, Sensors Actuat. B Chem. 129 (2008) 799–810.
[46] R. Hajian, E. Ekhlasi, R. Daneshvar, E J. Chem. 9 (2012) 1587–1598.
[47] K. Padmapriya, R. Barthwal, Biophys. Chem. 219 (2016) 49–58.
[48] X. Yang, G.L. Shen, R.Q. Yu, Microchem, J. 62 (1999) 394–404.
[49] Z. Xu, G. Bai, C. Dong, Bioorg. Med. Chem. 13 (2005) 5694–5699.
[50] K. Mostafa, R. Ahmad, D.M. Mohamad, N.M. Ismail, A.A. Mahmoud, J. Iran, Chem. Soc. 11 (2014) 1147–1163.
[51] K. Maruyama, Y. Mishima, K. Minagawa, J. Motonaka, Anal. Chem. 74 (2002) 3698–3703.
[52] Q. Wang, X. Wang, Z. Yu, X. Yuan, K. Jiao, Int. J. Electrochem. Sci. 6 (2011) 5470–5481.
[53] K.W. Kohn, M.J. Waring, D. Glaubiger, C.A. Friedman, Cancer Res. 35 (1975) 71–76.
[54] H.A. Benesi, J.H. Hildebrand, J. Am. Chem. Soc. 71 (1949) 2703–2707.
[55] N. Shahabadi, A. Fatahi, J. Mol. Struct. 970 (2010) 90–95.
[56] N. Arshad, M. Ahmad, M.Z. Ashraf, H. Nadeem, J. Photochem, Photobiol. B Biol. 138 (2014) 331–346.
[57] H.M. Berman, S. Neidle, C. Zimmer, H. Thurm, Biochim. Biophys. Acta 561 (1979) 124–131.
[58] A. Leo, C. Hansch, D. Elkins, Chem. Rev. 71 (1971) 525–616.
[59] P. Politzer, P. Lane, M.C. Concha, et al., J. Mol. Model. 13 (2007) 305–311.
[60] S. Riahi, S. Eynollahi, M.R. Ganjali, P. Norouzi, Int. J. Electrochem. Sci. 5 (2010) 1151–1163.